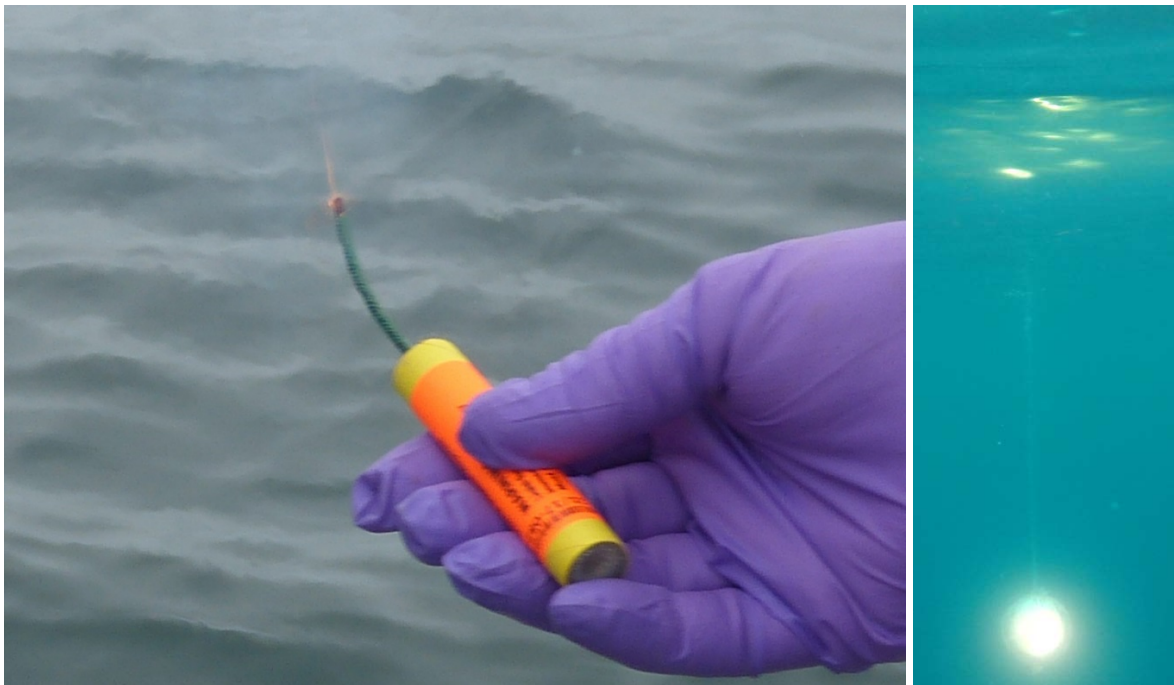




Seal Bomb Sound Source Characterization

Sean M. Wiggins, Anna Krumpel, LeRoy M. Dorman, John A. Hildebrand,
and Simone Baumann-Pickering

*Marine Physical Laboratory
Scripps Institution of Oceanography
University of California San Diego
La Jolla, CA 92037*



Suggested Citation:

Wiggins, S. M, Krumpel, A., Dorman L. M., Hildebrand, J. A., Baumann-Pickering, S. “Seal Bomb Sound Source Characterization,” Marine Physical Laboratory, Scripps Institution of Oceanography, University of California San Diego, La Jolla, CA, MPL Technical Memorandum 633 February 2019. Report submitted to and funded by National Oceanic and Atmospheric Administration (NOAA) National Marine Fisheries Service (NMFS) under Cooperative Agreement Grant No. NA15OAR4320071 Amendment 101. Experiment funding provided by Okeanos Foundation for the Sea. Experiment conducted under US Department of Justice (DOJ) Bureau of Alcohol, Tobacco, Firearms and Explosives (ATF) Federal Explosives license/permit No. 9-CA-073-33-0M-02140.

Cover photos: Ignited seal bomb (left); seal bomb underwater explosion (right). Photos by A. Krumpel.

Table of Contents

Abstract.....	1
Introduction.....	2
Methods	2
Experiment Overview	2
Seal bombs	4
Underwater Recordings.....	5
Impulse metrics.....	8
Source level estimation	8
Sound speed profile.....	9
High explosive modeling	9
Results.....	12
Example single nearby shot	12
Received SPL vs range	15
Refraction.....	16
Estimated source SPL	19
Discussion and Conclusions	20
Acknowledgements.....	21
References.....	22

List of Figures

Figure 1. Bathymetric map of experiment area offshore of La Jolla, California.	3
Figure 2. Seal bomb – Stoneco Energetics System, LLC Seal Cracker Device.	5
Figure 3. Autonomous acoustic recorder mooring configuration.	7
Figure 4. Sound pressure impulse waveform for high explosive model.....	11
Figure 5. Received sound pressure waveform for close range (262 m) seal bomb shot.....	13
Figure 6. Sound pressure impulse waveform from recorded seal bomb explosion at CPA.....	14
Figure 7. Seal bomb shot peak received SPLs vs logarithm base-10 ranges.	16
Figure 8. Sound speed and temperature profiles for study area.	17
Figure 9. Raypaths traced in two models with different sound speed profiles.	18

List of Tables

Table 1. Autonomous acoustic recorder nominal locations for three deployments.	3
Table 2. High explosive SPL and SEL (charge weight 2.33 g of 80% TNT-equivalent) @ 262 m.	11
Table 3. Seal bomb experiment days, deployed, unexploded, and detected.	12
Table 4. Seal bomb SPL and SEL with charge weight of 2.33 g at CPA (i.e., 262 m range).....	14
Table 5. Source SPL and SEL estimates from seal bomb with charge weight of 2.33 g	19

Abstract

Over 600 seal bombs were exploded underwater ~10 nm offshore of La Jolla, California during the late spring in 2017 to characterize their source signature, primarily focusing on source sound pressure level (SL). Calibrated underwater recordings of pulse waveforms were evaluated with regard to propagation environments so that appropriate transmission loss models could be used for SL estimates. For a hydrophone at 265 m depth, waveform refraction became important after about 1500 m slant range with approximately spherical spreading losses observed at shorter ranges. Peak SL for seal bombs was estimated to be 234 dB_p re 1 μPa @ 1m, along with three types of rms SL: 233, 230, and 226 dB_{rms} re 1 μPa @ 1m for -3dB and -10dB below peak and 90% energy rms types, respectively. For impulses such as explosions, these metrics are inadequate in fully describing the signal because pulse width is not properly accounted. Better metrics integrate over the pulse duration, accounting for the total energy in the pulse, including impulse sound pressure level, estimated as 83 dB re 1 μPa-s @ 1m, and sound exposure level (SEL) estimated as 197 dB re 1 μPa²-s @ 1m. In addition to utilizing proper transmission loss models with source levels for impact studies, additional accounting of energy from sea surface reflections and explosion bubble pulses should be considered, including calculating cumulative SEL over the entire period of event activity.

Introduction

Seal bombs, also known as acoustic harassment, wildlife control, and seal deterrent devices among others, are hand-thrown pyrotechnic devices capable of exploding underwater and used as a means to deter marine mammals during fishing operations. For example, seal bombs have been used at least as early as 1980 in the eastern tropical Pacific (ETP) yellow fin tuna purse-seine fishery to control dolphin swimming direction during all stages of net setting (Cassano *et al.*, 1990). More recently, opportunistic underwater recordings of thousands of explosions per month have been spatially and temporally correlated with commercial landings data of California market squid, suggesting seal bomb use during fishing operations to deter pinniped predation (Meyer-Löbbecke *et al.*, 2016).

A primary concern with the use of seal bombs is potential harm to marine mammals, especially for animals in close proximity to the explosions. While non-hearing physical damage is estimated for close ranges (<4 m; Myrick *et al.*, 1990a), hearing related injuries such as temporary threshold shift and permanent threshold shift or loss of hearing may occur at more distant ranges (e.g., Finneran, 2015). Furthermore, behavioral responses to explosions of the targeted animals, in addition to non-targeted marine mammals, may cause harm by altering biologically significant behaviors such as foraging or mating (e.g., Southall *et al.*, 2007).

Seal bomb source characterization is needed to provide metrics for managing marine noise pollution and mitigating effects on marine mammals due to high sound pressure levels from these explosions. In this report, we describe an experiment offshore of Southern California in which seal bombs were deployed and exploded at various ranges from an underwater recorder. Recordings of the received sound pressure waveforms were analyzed, and various metrics were measured and estimated to provide a characterization of the seal bomb source, including source sound pressure level, an important metric used for marine noise pollution management.

Methods

Experiment Overview

In late spring 2017, offshore of Southern California more than 600 seal bombs were individually exploded underwater over three days and recorded with an autonomous hydrophone at various ranges from less than 300 m to more than 8 km. The free-floating autonomous acoustic recorder was deployed a few hundred meters beneath the sea surface on 30 May, 1, and 2 June about 9 – 13 nm off the coast of La Jolla, California above seafloor depths ranging 635 – 870 m (Figure 1; Table 1). Global positioning system (GPS) receivers were attached to both the seal bomb deployment ship, Scripps Institution of Oceanography Research Vessel (R/V) Saikhon, and a sea surface float above the hydrophone to provide source-receiver ranges. These ranges along with measured sound pressure levels at the hydrophone receiver provide the measures needed to estimate seal bomb source sound pressure levels.

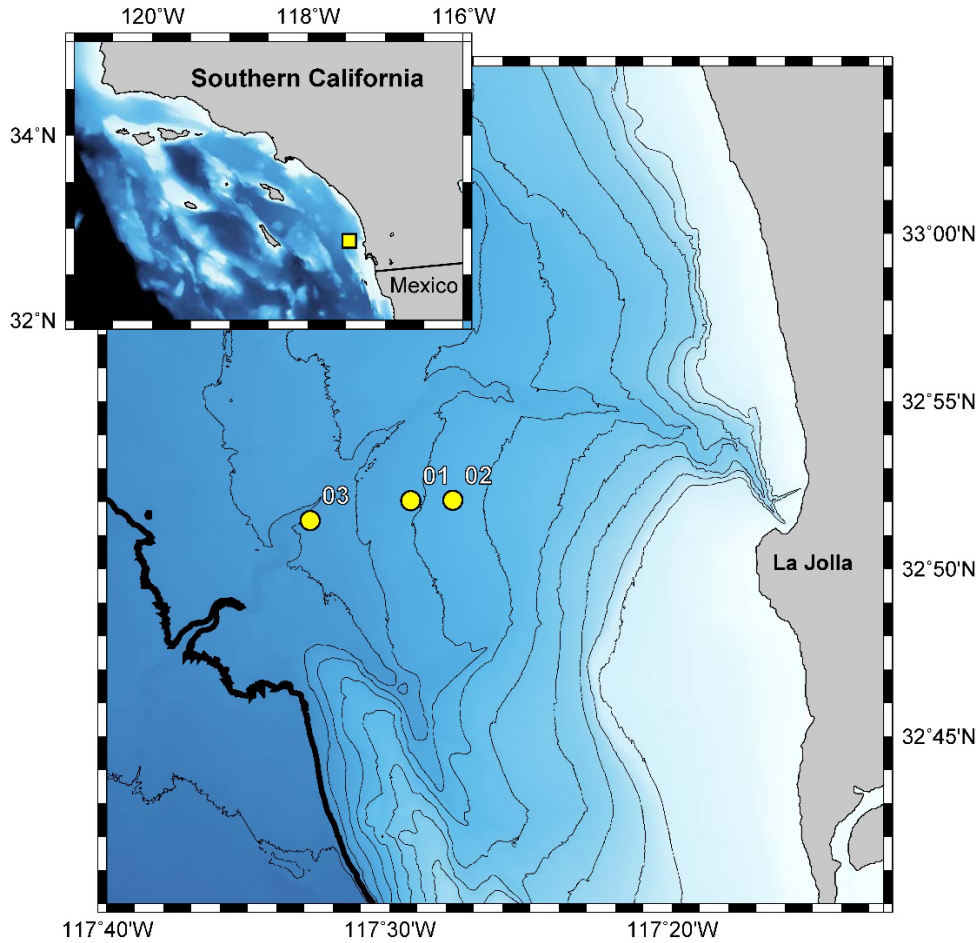


Figure 1. Bathymetric map of experiment area offshore of La Jolla, California. Inset map yellow square is the study area. Yellow circles 01, 02, and 03 are autonomous hydrophone deployment sites for 30 May, 1 and 2 June 2017, respectively. Thick contour is 1000 m depth, with thin contours at 100 m increments. Dark colors are deeper and farther offshore.

Table 1. Autonomous acoustic recorder nominal locations for three deployments. Deployment number, date, latitude, longitude, hydrophone depth, and seafloor depth.

Deployment Number	Date	Latitude (N)	Longitude (W)	Hydrophone Depth (m)	Seafloor Depth (m)
01	30 May, 2017	32° 52.034'	117° 29.235'	265	715
02	1 June, 2017	32° 52.052'	117° 27.750'	265	635
03	2 June, 2017	32° 51.443'	117° 32.802'	265	870

Seal bombs

In pyrotechnics, a firework that generates a loud report (i.e., bang), often along with a bright flash, is a salute. Typically, the explosive material used in salutes is flash powder, a low explosive that deflagrates (i.e., burns and builds up and then decreases pressure over time of the explosion), but at a much faster rate than black powder. This should not be confused with detonation of high explosives, such as trinitrotoluene (TNT), where a shock wave (i.e., a wave front traveling faster than the speed of sound) is generated and maximum pressure is instantaneous but decays quickly and exponentially.

Salutes come in many sizes, from small 2.5 cm diameter spherical cherry bombs with ~1 g of flash powder to much larger and more powerful cylinders or sticks with 50-100 g of flash powder. Seal bomb salutes are cylindrical with a fuse protruding from one of the ends. There are different seal bomb manufacturers around the world using various amounts (~2 – 6 g) and different formulations of flash powder (Myrick *et al.*, 1990b).

This study was limited to just one type of seal bomb, the Seal Cracker Device manufactured by Stoneco Energetics Systems LLC, Prescott Valley, Arizona, United States of America. The Seal Cracker Devices, from here onward referred to as seal bombs, used were ~8.3 cm long x 1.7 cm diameter cardboard tubes wrapped with yellow paper and a bright orange label with a ~6.7 cm long x 0.3 cm diameter green fuse protruding from one of the plastic-plug sealed ends (Figure 2a). Inside the tube were two chambers: a lower one with silica sand used to provide weight so that the seal bomb will sink upon deployment, and an upper one containing flash powder and the unlit end of the fuse for deflagration initiation (Figure 2b). The fuse was a visco fuse with a black powder core and coated with nitrocellulose for water resistance so that it will continue to burn after deployment, underwater. The fuse burn duration before explosion was about 8 seconds. Explosion depths were estimated to be 1 – 4 m (Myrick *et al.*, 1990b).

The seal bombs used in this study had a charge weight of 2.33 g flash powder using a standard formulation of about 64.0% potassium perchlorate (KClO₄) as the oxidizer and a fuel of 25% aluminum powder and 10% sulfur (personal communications M. Stonebraker, Stoneco Energetics Systems). This charge weight is similar to common M-80 salutes.

During the experiment, the free-end of the seal bomb fuse was ignited using a standard home-improvement-style push-button torch hose kit connected to a 14 oz. bottle of propane. After ignition, the seal bomb was tossed by hand into the water 5 - 10 m starboard and off the rear quarter of the R/V Saikhon while underway at ~6 kts. Seal bombs were deployed approximately every 30 s along a transit line, marked with the ship's GPS. Notes were logged for each seal bomb deployment including time, location, and type of explosion: good, dud, shallow; along with changes in deployment schedule due to deviations in ship track or pauses during marine mammals, fish, or birds presence.

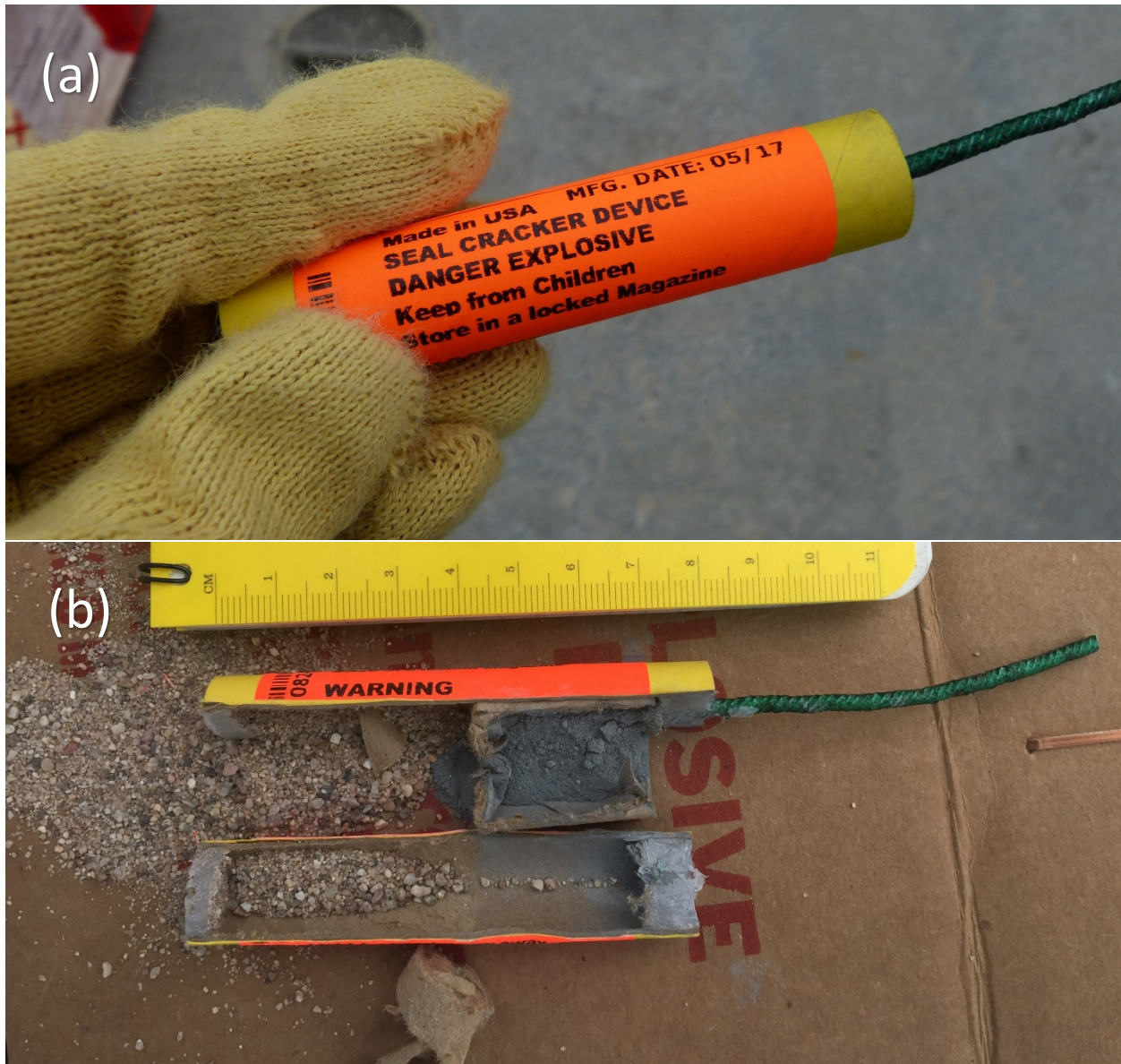


Figure 2. Seal bomb – Stoneco Energetics System, LLC Seal Cracker Device. (a) Seal bomb prior to ignition and deployment. (B) Seal bomb cut long-axis shows internal contents with two chambers: silica sand for sinking weight, and gray flash powder with green fuse for underwater explosion.

Underwater Recordings

To measure sound pressure levels of seal bomb explosions, recordings were made using an autonomous High-frequency Acoustic Recording Package (HARP - Wiggins and Hildebrand, 2007). The HARP was configured to record at 200 kHz sample rate with 16-bit samples onto laptop computer type hard disk drives. Because seal bombs generate high sound pressure levels and some source-receiver ranges were relatively short, the sensitivity of the hydrophone was

reduced from standard HARP hydrophones by about 40 decibels (dB) to prevent signal clipping. The hydrophone was constructed of two sensors: Benthos AQ-1 for frequencies below 10 kHz and International Transducer Corporation 1042 for frequencies above. The sensors are specified as having approximately the same sensitivity of -201 dB re 1 V/ μ Pa. The hydrophone signal conditioning electronics gain was set to be 10 dB and full band 10 Hz – 100 kHz response was calibrated in our lab at Scripps Institution of Oceanography so that absolute received sound pressure levels could be measured. During the experiment, we also towed ~10 m aft of the R/V Saikhon's port quarter a hydrophone array with sensor configuration similar to the HARP, and even though the recorded signals were clipped, precise signal timing information was obtained.

Typically, HARPs are deployed on the seafloor as bottom-mounted instruments or in a mooring configuration including an acoustic release system used for jettisoning ballast weight and instrument retrieval. For this study, the data logger housing and hydrophone were suspended beneath the sea surface in a multiple float and weight system such that the hydrophone was decoupled from vibrations and motions incurred by the sea surface float (Figure 3). The hydrophone was placed at 265 m depth, well below of the thermocline to avoid acoustic raypath refraction problems. Attached to a flag pole on the sea surface float about 1.5 m above the waterline in a plastic bag was a dog collar GPS (Garmin Astro 32 with T5). The dog collar transmitted positions every 2 minutes via radio frequencies to its receiver onboard the R/V Saikhon for logging. Float drift rate was less than 0.1 kts. The receiver for the dog collar also was used to record the ship GPS positions.

After recovery of the recorder, the hard disk drives were removed, and disk image files of raw data disks were generated for archiving and processing. Processing raw data into working data included uncompressing and creating multiple 37.5-minute audio (wav format) files with high precision time stamps. The audio files were used to make long spectrograms to provide a graphical index for the data allowing quick and easy access to sound events of interest (see the acoustic analysis software package, *Triton* - Wiggins and Hildebrand, 2007).

Software was developed in MATLAB (Mathworks, Inc., Natick, MA, USA), a high-level programming language and numerical analysis environment, to filter, automatically detect, measure amplitudes, and save snippets of received seal bomb shots from the audio files. An 8th order Chebyshev type 2 low-pass filter (LPF) with a stopband edge at 10 kHz was used on the waveforms to reduce apparent high-frequency transient effects from the hydrophone. The detector was a simple energy detector with the 0-peak threshold set to ~16 Pa (144 dB re 1 μ Pa) to identify pulse first arrival times. Snippet waveforms from 0.1 s before detection to 1.0 s after detection were saved as MATLAB binary files. Additional software was developed to evaluate seal bomb shots, including metric calculations and plots.

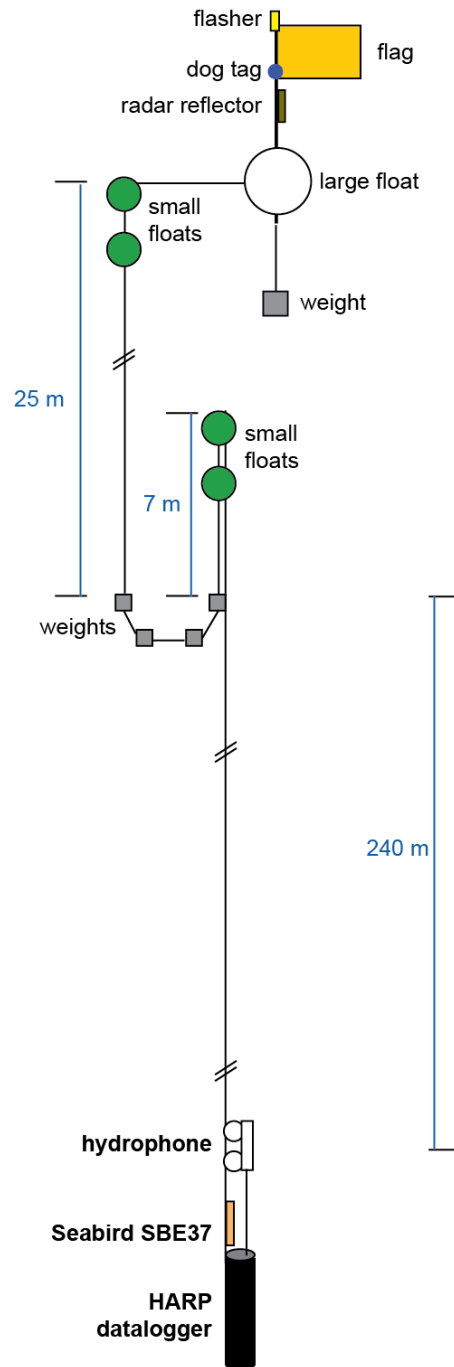


Figure 3. Autonomous acoustic recorder mooring configuration. The large white float was at the sea surface and included a flag, flasher and radar reflector to prevent being struck by nearby transiting vessels. Also attached to the flag was a dog tag GPS receiver which transmitted locations back to R/V Saikhon. Beneath the sea surface on the mooring line was a system of floats and weights to decouple the sea surface motion from the hydrophone at 265 m depth. Hydrophone depth was confirm via Seabird temperature-pressure logger.

Impulse metrics

Different metrics are used to describe different types of sound pressure signals. For example, continuous pressure wave signals from sources such as ships and sonar pings are typically reported as root-mean-square (rms) of the pressure, $p(t)$, over a time window, T :

$$P_{rms} = \sqrt{\frac{1}{T} \int_0^T p^2(t) dt} \quad (1)$$

where the time window is typically defined as the signal width 3 dB down from the peak level, the signal width 10 dB down from the peak level, or from 5% to 95% of the signal's total energy; typically described as -3dB, -10dB, and 90% rms, respectively. Impulsive sounds are usually not well-represented as rms because rms depends on the analysis window, which for transient signals is critical (e.g., Madsen, 2005). For example, the rms for a given impulse is typically lower for 90% than -3dB because of a longer time window for the 90% rms metric.

Impulsive or transient sounds, such as those from seismic air guns or underwater explosions, are often described as peak (p) or peak-to-peak (pp) pressures; however, these metrics do not account for different pulse shapes and durations. The energy flux density, with units $\text{Pa}^2 \cdot \text{s}$, accounts for the shape of the pulse and provides a useful comparable metric for transient signals by integrating the squared-pressure of the pulse waveform time series over a time window:

$$E = \int_0^T p^2(t) dt \quad (2)$$

Another useful and comparable metric for transient signals is the positive acoustic impulse, or impulse pressure, with units $\text{Pa} \cdot \text{s}$. The positive impulse is often used for studies on the effects of explosions on animals (Richardson *et al.*, 1995) and is the integral of pressure over duration of the pulse:

$$P_i = \int_0^T p(t) dt \quad (3)$$

Because these metrics vary by large amounts, they are often presented as dBs. To convert peak and rms pressures to dB sound pressure levels (SPLs), 10 times the base-10 logarithm of the squared pressure was used, or $SPL = 20 \log_{10}(P)$. Similarly, for the energy flux density and the impulse pressure, the sound exposure level (SEL) was calculated as $SEL = 10 \log_{10}(E)$ and the impulse SPL = $10 \log_{10}(P_i)$.

Source level estimation

Source sound pressure level is rarely measured in the field directly as it is typically referenced at 1 m range, which can be prohibitively close to the source, introducing complexities associated with the near field acoustic environment. Instead, received sound pressure levels (RLs) are measured at ranges greater than 1 m and range-dependent corrections for acoustic propagation (i.e., transmission loss, TL) are applied to estimate source sound pressure levels (SLs) at 1 m via the sonar equation:

$$SL = RL + TL \quad (4)$$

where values are in dB units (Urlick, 1983). Often, TL is a linear function of the base-10 logarithm of range such that

$$TL = X \log_{10}(\text{range}) \quad (5)$$

where TL has units dB re 1 m, range has units m, and X is the regression coefficient, or slope, of a linear regression model of RL versus $\log_{10}(\text{range})$.

Estimating source sound pressure levels from acoustic waves that propagate along straight-paths is typically much less complicated than from raypaths with additional energy loss from refraction, reflections, and absorption. For example, the sound pressure loss in a homogenous, unbounded and non-absorptive medium from a source radiating outward equally in all directions is termed spherical spreading and $X = 20$ in Eq. (5) for short ranges and low frequencies (e.g., Urlick, 1983). When the medium is bounded by top and bottom parallel planes, sound is reflected off of the planes and spreads cylindrically, propagating in a waveguide, resulting in a lower transmission loss with $X = 10$; however, additional losses at the bounding planes can occur due to surface roughness scattering, waveform destructive interference and, in the case of the seafloor boundary, refraction into substructure. Water column refraction can increase or decrease transmission losses via focusing or defocusing sound waves as they bend toward or away from a receiver in a non-homogenous medium.

Sound speed profile

The speed of sound in the ocean typically varies with depth which affects how sound travels from source to receiver, including causing sound raypath refraction (i.e., bending) and creating shadow zone regions where direct raypaths cannot reach. Sound speed is a function of salinity, temperature, and pressure, with the latter two metrics having the largest effect through the water column. Temperature and pressure were measured and recorded using a Seabird SBE-39 attached to the line between the data logger pressure housing and the hydrophone (Figure 3). This configuration provided two casts per deployment day, one down when the recorder was deployed and one up when the recorder was recovered. The three days of recording provided 6 casts, which were averaged to provide an overall mean temperature profile for the experiment. This temperature profile was used to estimate the mean sound speed profile using the Chen and Millero (1977) approach with a constant 35 ‰ salinity.

The sound speed profile was used to evaluate how raypaths travel between source and receiver in the area of the experiment. To estimate raypaths from source to receiver we used BELLHOP, a ray tracing model software program run in MATLAB (Porter, 2011) along with the mean sound speed profile.

High explosive modeling

While flash powder in seal bombs deflagrates and does not detonate, high explosives have been well-studied (Cole, 1948) and provide useful comparisons. As a high explosive detonates, it

creates a shock wave with which the pressure can be approximated as exponentially decaying over time:

$$p(t) = p_0 e^{-t/t_0} \quad (7)$$

where $p(t)$ is the instantaneous pressure at time t after the beginning of the shock wave, p_0 is the peak pressure at time $t = 0$, and t_0 is the exponential time constant $p_0/e = 0.368p_0$.

Urlick (1983) summarizes (Arons *et al.*, 1949) semi-empirical work (and converted to metric units here) which found a power law relationship between peak pressure in μPa , charge weight (W) in kg, and range (R) in m such that

$$p_0 = k \left(\frac{W^{1/3}}{R} \right)^\alpha \quad (8)$$

where, for TNT, $k = 5.24 \times 10^{13}$ and $\alpha = 1.13$. Similarly, the time constant, in microseconds, power law relationship to charge weight and range for TNT was found to be

$$t_0 = 92.5 W^{1/3} \left(\frac{W^{1/3}}{R} \right)^{-0.22} \quad (9)$$

After the detonation, a globular mass of gaseous material is formed, expands, and then collapses creating a secondary pressure pulse, or bubble pulse. Successive oscillations create additional bubble pulses, but with lower pressures, at shallower depths than preceding pulses. The time interval, T_i in s, between the detonation and first bubble pulses was empirically found to be

$$T_i = \frac{0.48KW^{1/3}}{(d+10)^{5/6}} \quad (10)$$

where, $K = 4.36$ for TNT and d is depth below sea surface in m. Arons (1954) noted that these empirical relationships for high explosives (converted to metric units) are valid up to ranges of

$$R_{\max} \approx 793W^{1/3} \quad (11)$$

Note that α in the range-dependent Eq. (8) is greater than unity, which results in a TL coefficient $X = 22.6$ when the peak pressure is converted to SPL via $20\log_{10}(p_0)$. This loss, along with the -0.22 exponent in Eq. (9), shows an additional attenuation of the peak pressure and broadening of the shockwave pulse as it decays with increasing range, which is due to nonlinearity of the underwater medium (e.g., Beyer, 1974).

As an example and for comparison with our measured values for seal bomb explosions, we use the seal bomb charge weight of 2.33 g with an 80% mass TNT-equivalent (Myrick *et al.*, 1990b) and range of 262 m (i.e., closest range in our experiment), although this range is beyond the valid maximum range (~ 100 m) from Eq. (11) for the relatively small seal bomb charge weight. Eqs. (8) and (9) were used to estimate maximum (peak) SPL and pressure decay time constant, and the waveform Eq. (7) was used for estimating impulse SPL and SEL using the trapezoidal rule for numerical integration, and three types of rms SPLs including time window durations (Table 2; Figure 4). The bubble pulse time interval from Eq. (10) is 30 ms.

Table 2. High explosive SPL and SEL (charge weight 2.33 g of 80% TNT-equivalent) @ 262 m.

Metric	Levels	Time constant/window (μs)
Peak SPL	199 (dB_p re 1 μPa)	61
rms-3dB SPL	198 (dB_{rms} re 1 μPa)	21
rms-10dB SPL	195 (dB_{rms} re 1 μPa)	70
rms90% SPL	191 (dB_{rms} re 1 μPa)	179
Impulse SPL	57 (dB re 1 $\mu\text{Pa}\cdot\text{s}$)	500
SEL	154 (dB re 1 $\mu\text{Pa}^2\cdot\text{s}$)	500

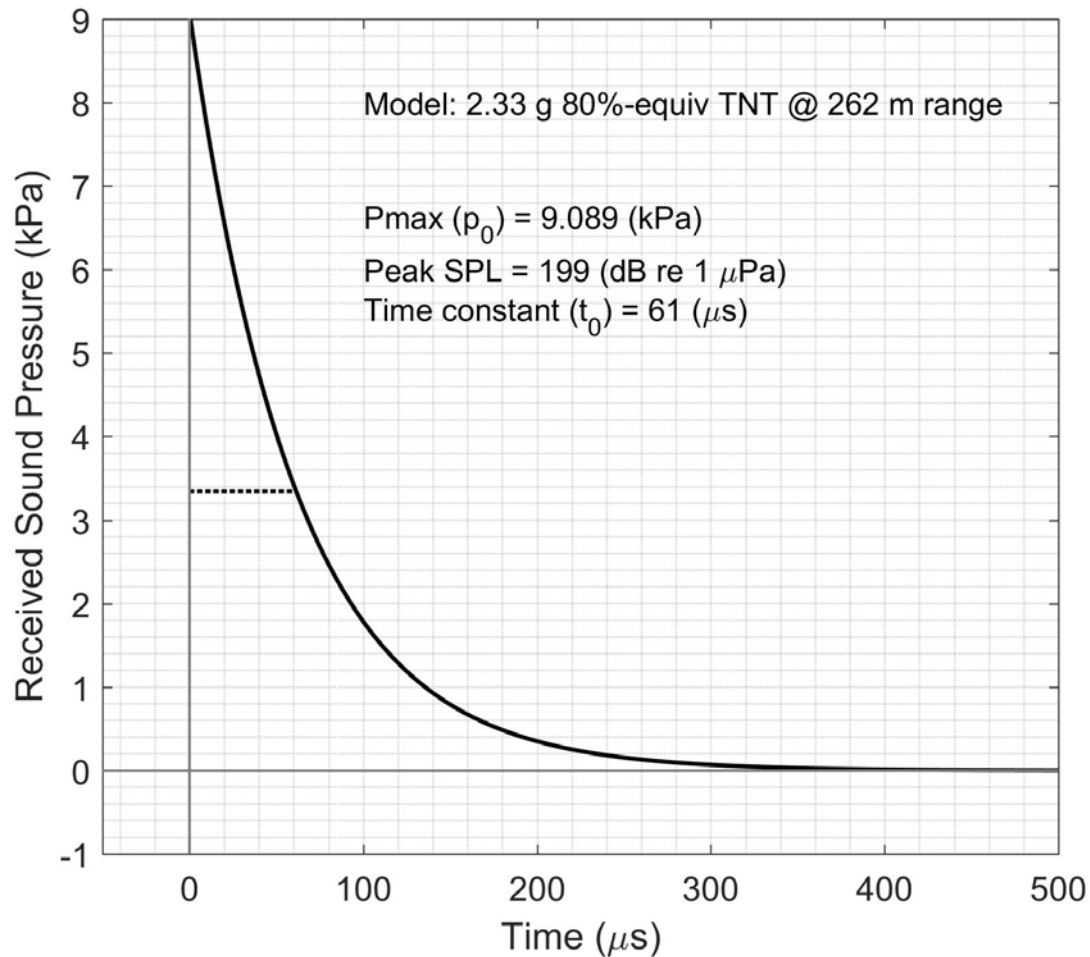


Figure 4. Sound pressure impulse waveform for high explosive model. Model from Eq. (7) used 2.33 g of 80% mass equivalent TNT at 262 m range along with calculated metrics from Eqs. (8) – (10). Dotted line is for time constant, t_0 , at 3.34 kPa.

Results

Over the three experiment days, 648 seal bombs were deployed, 46 were logged as unexploded, and 542 were detected with the automatic detector (Table 3). Unexploded seal bombs may not have been lit properly, or had some other fault with the fuse or explosive. Seal bombs that were not detected either did not explode or likely had received sound pressure levels lower than the detector threshold due to sound propagation limitations such as long range or very shallow explosion depths (i.e., near the sea surface pressure release boundary).

Table 3. Seal bomb experiment days, deployed, unexploded, and detected.

Experiment Day	01	02	03	Total
Date	05/30/2017	06/01/2017	06/02/2017	3 days
Deployed Seal Bombs	144	288	216	648
Unexploded Seal Bombs	18	19	9	46
Detected Seal Bombs	91	245	206	542

Example single nearby shot

Seal bomb shots near the hydrophone receiver provided the highest received levels and best signal-to-noise ratio (SNR) for evaluating the arriving pulses. For example, a LPF shot from the closest point of approach (CPA), where the explosion was nearly directly above the hydrophone on 2 June 2017, clearly shows four distinct pulses within the first 75 ms (Figure 5). The direct arrival from the shot, ~262 m from the hydrophone, was a steep rising and slower decaying pulse which was then reflected off the sea surface causing a phase reversal and resulting negative pulse (Figure 5 a). At about 37 ms after the first arrival, the first bubble pulse peaked, but with a slower rise time than the direct pulse, which was also reflected off of the sea surface (Figure 5 b). The third positive and negative pulses from the second bubble pulse had the same initial steep character and phase as the first pulse and its sea surface reflection (SSR) (Figure 5 c). The third bubble pulse and its SSR arrived ~69 ms after the direct pulse and at lower amplitude than the first two bubble pulses. All SSR were around 4 ms after preceding positive pulses, indicating an approximate shot depth of 3 m using a nominal 1500 m s^{-1} sound speed. The time difference between the positive pulse and its SSR for the third bubble pulse was ~0.25 ms less than for the first bubble pulse indicating the third bubble pulse was shallower than the first. In general with all recorded shots, the time between the direct first pulse arrival and the bubble pulses varied by a few milliseconds showing slight variability in shot depth (Eq. 10).

A more detailed evaluation of the first 2 ms from the CPA seal bomb shot (Figure 6) allows for comparison to the example high explosive model shot with higher pressure and shorter duration (Figure 4). The seal bomb unfiltered (dotted) waveform shows a leading transient with positive and negative pulses 30 μs apart which we attribute to the hydrophone electronics. These transients only occurred on direct and the second bubble pulses, likely due to their higher

frequency content than the first and third bubble pulses, and were most prominent for close shots, decreasing with range. The LPF (solid) waveform shows a reduction in high frequencies and the leading transient, but retains the pulse shape and area underneath the curve (i.e., impulse pressure, P_i) allowing various metrics to be calculated (Table 4).

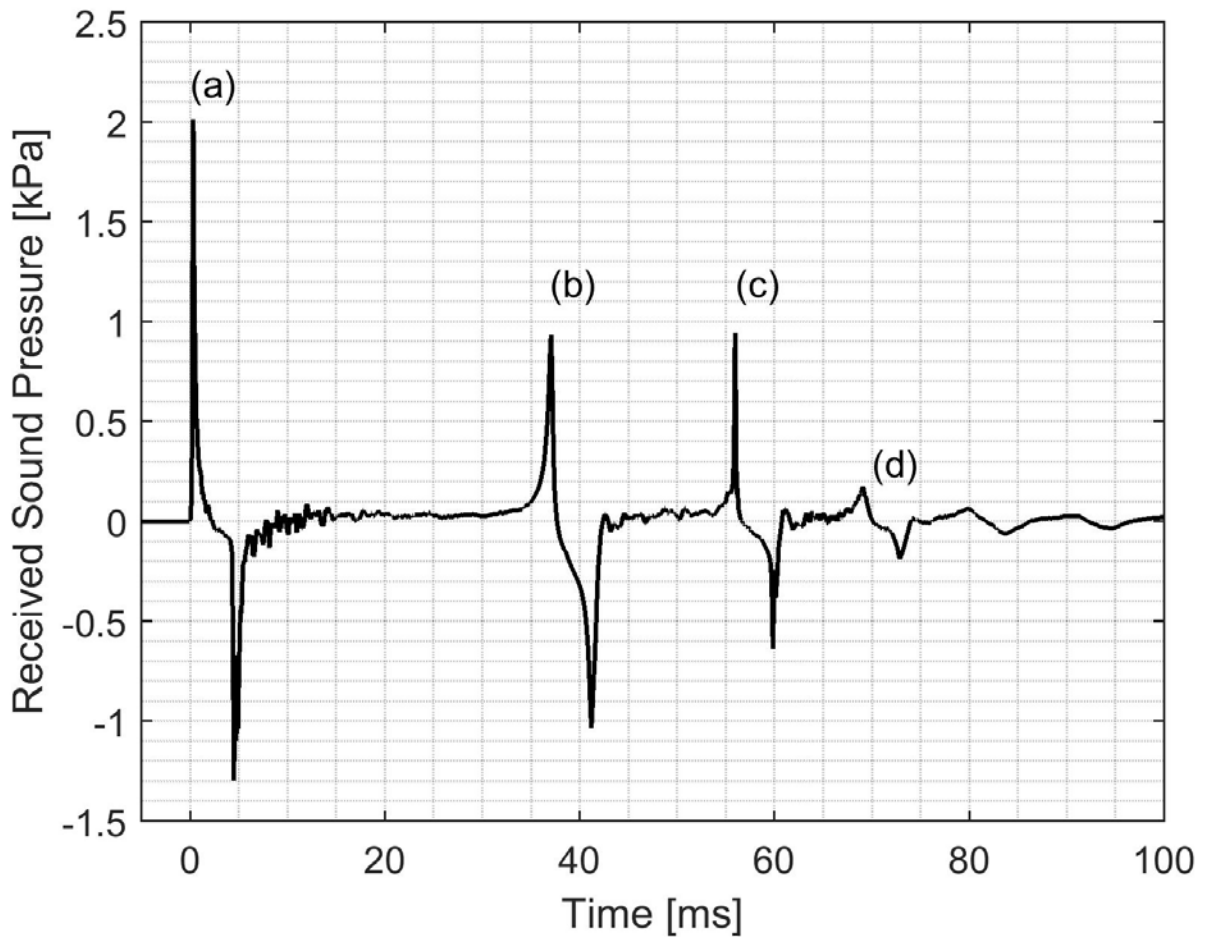


Figure 5. Received sound pressure waveform for close range (262 m) seal bomb shot. (a) Initial pressure wave (0 ms) and its sea surface reflection (SSR) (4 ms). (b) First bubble pulse (37 ms) and its SSR (41 ms), (c) second bubble pulse (56 ms) and its SSR (60 ms), (d) third bubble pulse (69 ms) and its SSR (73 ms). All SSR occurred ~ 4 ms after preceding arrivals indicating the explosion depth was 3 m using 1500 ms^{-1} sound speed.

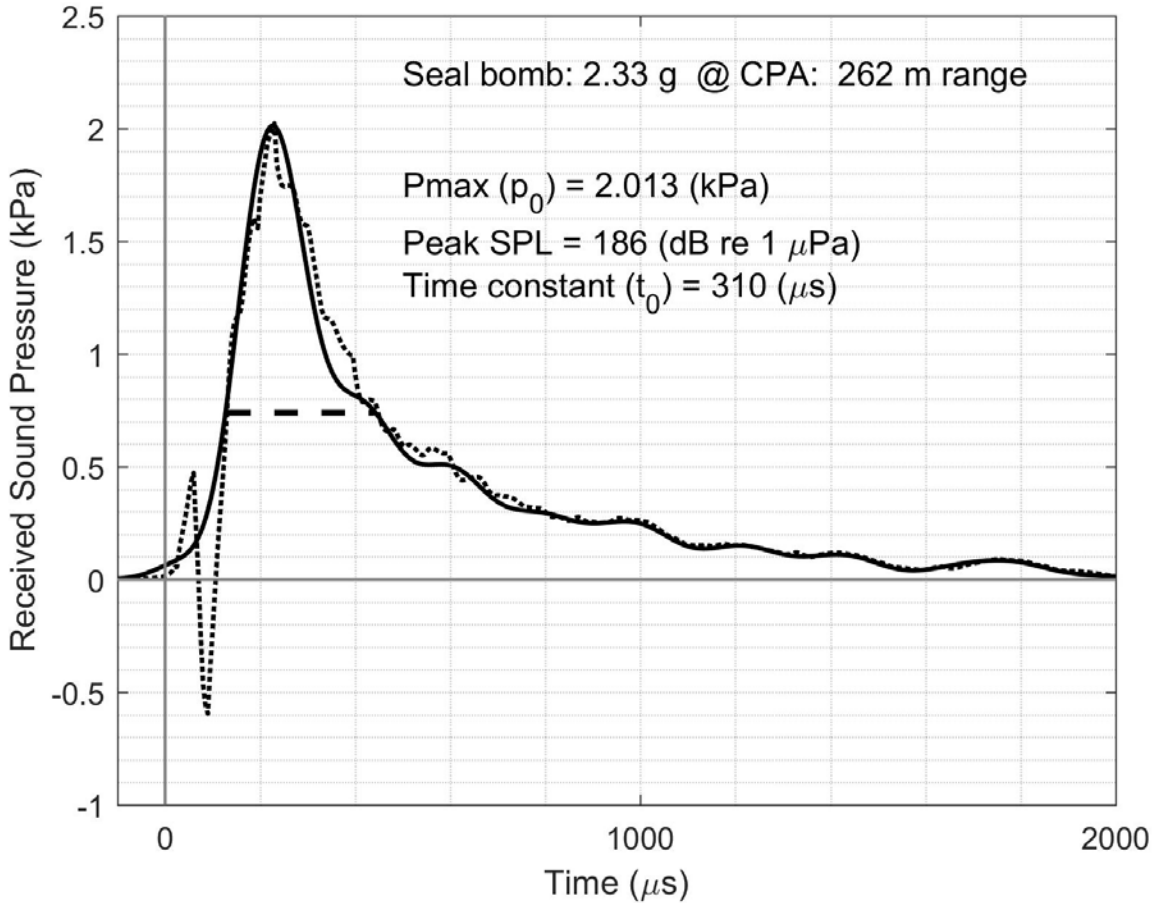


Figure 6. Sound pressure impulse waveform from recorded seal bomb explosion at CPA. Seal bomb with 2.33 g of flash powder was exploded at 262 m range from hydrophone receiver. P_{max} was measured from the waveform and the time constant (dashed horizontal line at 0.74 kPa) was calculated using P_{max} and Eq. (7). Dotted pulse is unfiltered; whereas, the solid pulse is filtered using an 8th order Chebyshev type 2 LPF with a stopband edge at 10 kHz to minimize hydrophone induced leading transient with positive and negative pulses.

Table 4. Seal bomb SPL and SEL with charge weight of 2.33 g at CPA (i.e., 262 m range).

Metric	Levels	Time constant/window (μs)
Peak SPL	186 (dB _p re 1 μPa)	310
rms-3dB SPL	185 (dB _{rms} re 1 μPa)	120
rms-10dB SPL	182 (dB _{rms} re 1 μPa)	350
rms90% SPL	178 (dB _{rms} re 1 μPa)	1095
Impulse SPL	59 (dB re 1 μPa·s)	2000
SEL	149 (dB re 1 μPa ² ·s)	2000

Comparison of the high explosive model (Table 2) and the measured seal bomb explosion at CPA (Table 4) shows peak and rms SPLs are 13 dB lower and time windows are 5 – 6 times longer for the seal bombs than the model; whereas, the time integrated metrics were more similar with the impulse SPL 2 dB higher and SEL 5 dB lower for the seal bomb.

Received SPL vs range

To examine our study area TL environment, measured peak received SPLs from seal bomb shots were plotted against their ranges using a base-10 logarithm scale (Figure 7). Three distinct regions grouped by ranges are apparent: low-loss (260 – 1200 m), high-loss (1200 – 2000 m), and variable-loss (2000 – 9000 m).

A linear regression model for SPL versus $\log_{10}(\text{range})$ for the low-loss, short-range region provides a slope, or regression coefficient, $X = 18$, which is slightly less lossy than spherical spreading, and the y-intercept, or regression error, suggests a SL of $\sim 230 \text{ dB}_p \text{ re } 1 \mu\text{Pa @ } 1 \text{ m}$. The coefficient of determination for this model was $R^2 = 0.95$ using $N = 101$ SPL-range pairs. Closer inspection of this region shows three sub-regions (260 – 340 m, 400 – 800 m, and 800 – 1200 m) each with slightly different and decreasing slopes of approximately 20, 19, and 17, respectively, becoming less lossy with increased range due to refraction focusing effects. Refraction is also the cause of the high losses in the region between 1200 and 2000 m, with defocusing creating a TL slope of $X \approx 130$ in a region where direct raypaths cannot reach. Greater than 2000 m range, the raypath arrivals are complicated by sound waves reflecting off the seafloor and sea surface, in some cases multiple times, and there is no clear range-dependency of TL, showing more than 10 dBs of SPL variability (Figure 7).

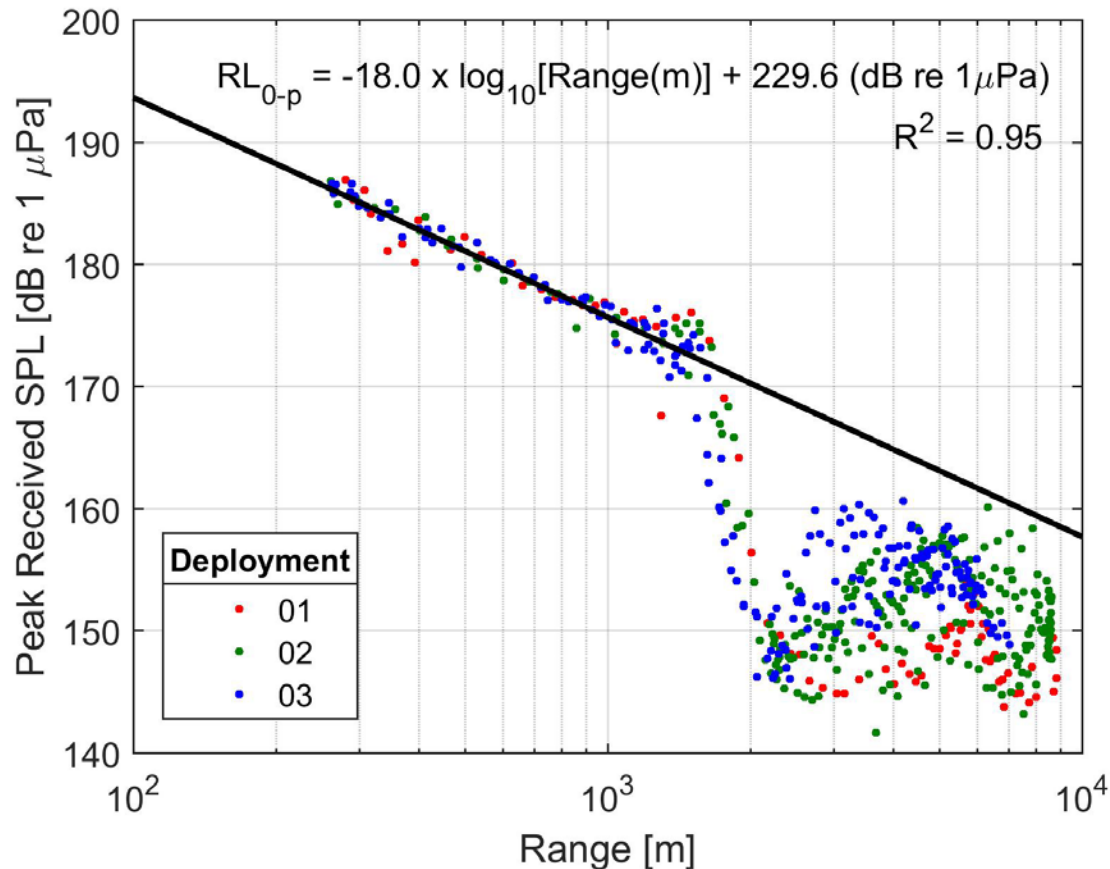


Figure 7. Seal bomb shot peak received SPLs vs logarithm base-10 ranges. Three distinct propagation regions: low-loss (260 – 1200 m), high-loss (1200 – 2000 m), and variable-loss (2000 – 9000 m). Dot colors represent deployment number. Linear regression model fit to the low-loss region (260 – 1200 m) shows less loss than spherical spreading with an extrapolated $SL \sim 230 \text{ dB}_p \text{ re } 1 \mu\text{Pa} @ 1 \text{ m}$ (regression error or y-intercept) and coefficient of determination, $R^2 = 0.95$.

Refraction

To better understand the slight decrease in TL as range increases from the CPA and then the large increase in loss around 1200 – 2000 m range shown in Figure 7, two-dimensional ray tracing in a depth-dependent sound speed model was performed and shows the effects of refraction. The sound speed profile for the model was estimated from an average of six depth-temperature casts during the experiment using the Chen and Millero (1977) approach (Figure 8).

The sound speed profile shows a large decrease in sound speed in the first ~20 m of depth, resulting in a large sound speed gradient or slowness ($\sim 1 \text{ s}^{-1}$) near the sea surface. The amount of raypath curvature (i.e., refraction) is directly related to the magnitude of the sound speed gradient with raypaths bending more in higher gradients environments away from high sound

speed and when traveling more perpendicular to the direction of the gradient. For example, a raypath initially traveling horizontally (perpendicular to the direction of the sound speed gradient) in the upper 10 m of this model will curve downward away from the sea surface such that a receiver at the same depth as the source will receive levels less than spherical spreading (i.e., defocusing) and a receiver at a deeper depth will receive levels greater than spherical spreading (i.e., focusing) for sufficiently close ranges.

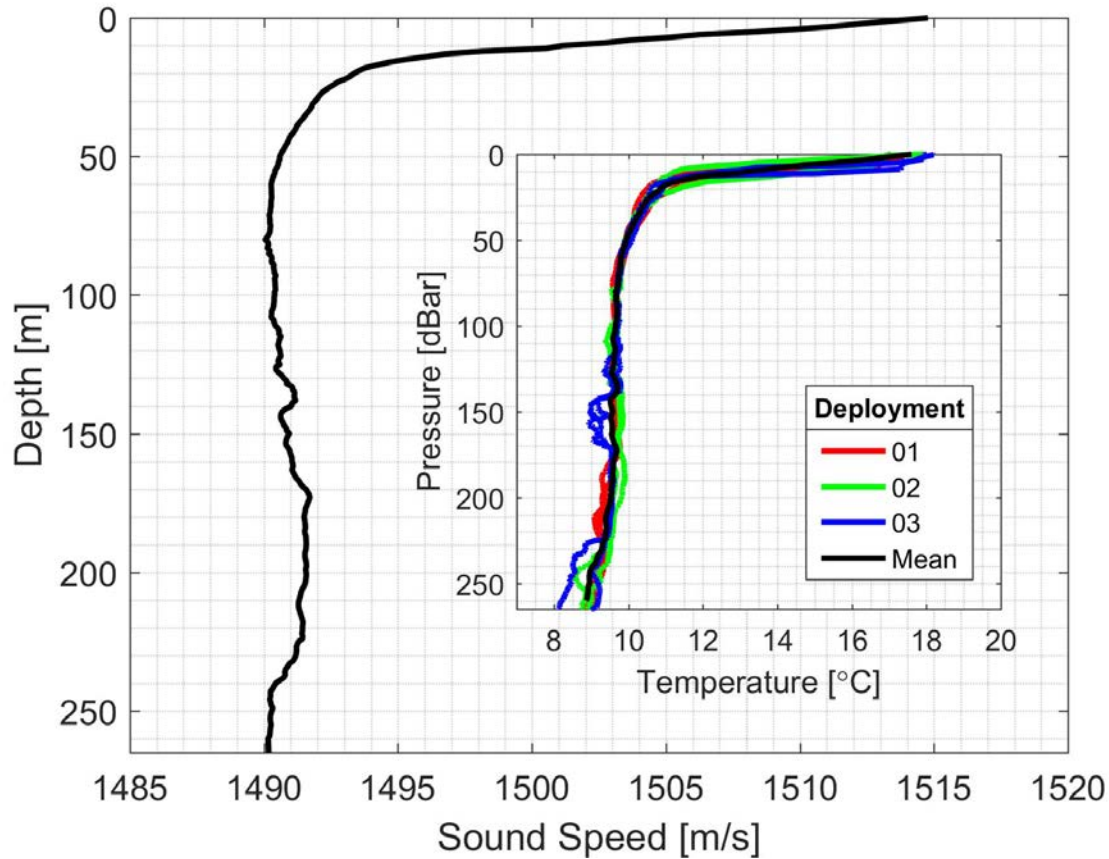


Figure 8. Sound speed and temperature profiles for study area. Sound speed profile was estimated based on the method of Chen and Millero (1977) using the mean (black line) temperature profile (inset) from two casts from each deployment (red, green, blue) and salinity of 35‰.

A graphical example of this refraction effect shows raypaths traced from a 3 m deep shot with angles relative to the sea surface from -3° to 45° in 2° increments for two sound speed profiles: the one used in this experiment and a homogenous 1500 m s^{-1} profile exhibiting spherical spreading. In the refraction model (Figure 9a) at the receiver depth (blue horizontal line), the area focusing raypaths can be seen at ranges greater than $\sim 1200 \text{ m}$ up until the last ray (shot toward the sea surface) $\sim 1700 \text{ m}$ range. Beyond 1700 m , a shadow zone results, an area void of raypaths with very high transmission losses. The homogenous sound speed model produces straight rays and no acoustic shadowing nor focusing (Figure 9b).

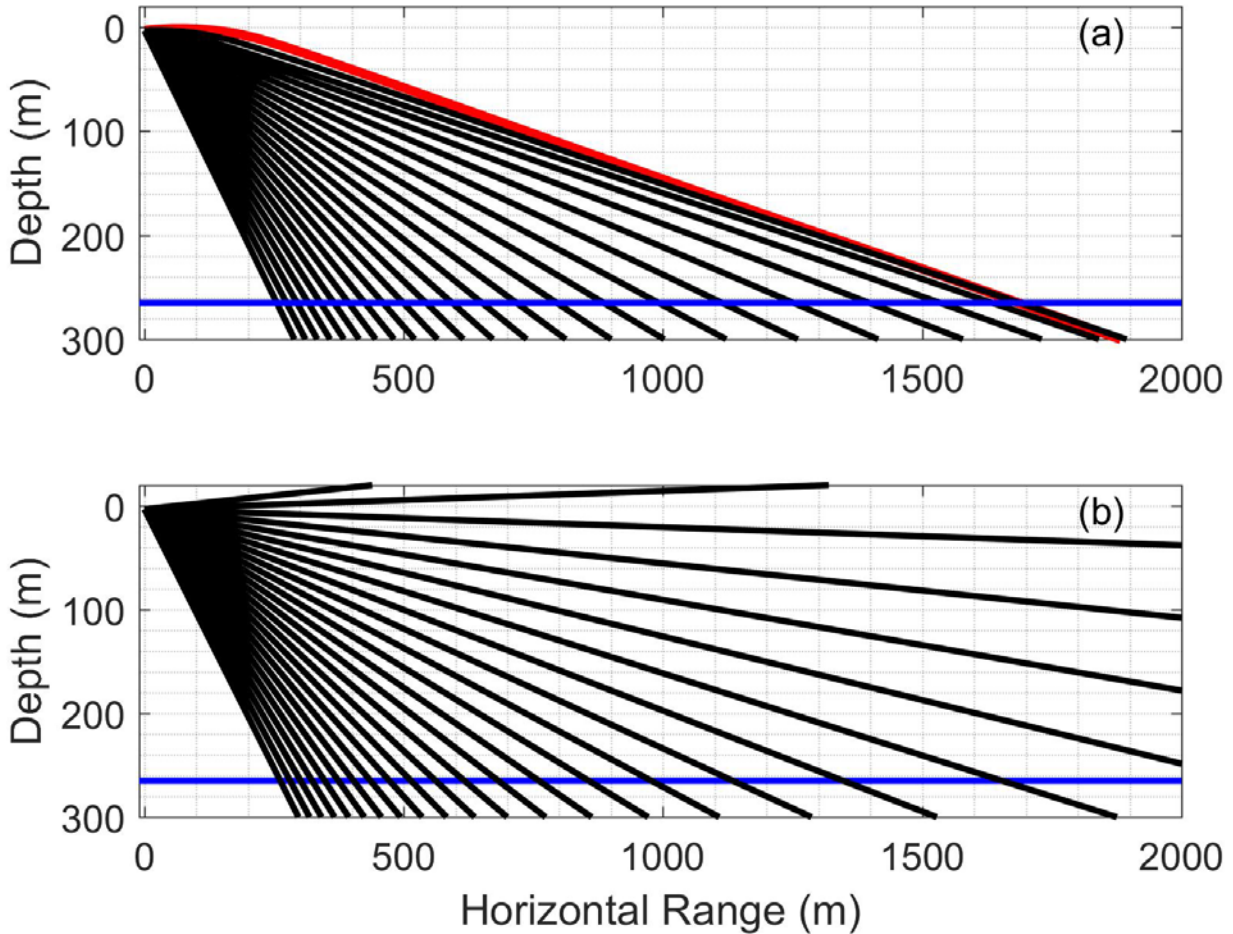


Figure 9. Raypaths traced in two models with different sound speed profiles. Rays were shot from a depth of 3 m in 2° increments from -3° to 45° relative to the sea surface. The blue horizontal line represents the hydrophone receiver at 265 m depth. (a) Sound speed profile from Figure 8 with a strong gradient near the sea surface creates strong refraction with rays becoming closer together as the range increases until the maximum range is reached (red raypath was shot toward surface at -3° , but refracted downward). (b) Homogenous sound speed throughout the model causes all raypaths to be straight and evenly spaced in angle without refraction-caused shadow or focusing zones. Note, depth and range are at different scales ($\sim 1:2$).

Estimated source SPL

To estimate seal bomb SLs (Table 5) from the sonar equation (Eq. 4), we used the RL measurements from the CPA shot at 262 m (Table 4) and a spherical spreading TL ($20\log_{10}(262 \text{ m}) = 48 \text{ dB re } 1 \text{ m}$ for the levels relative to pressure squared and $10\log_{10}(262 \text{ m}) = 24 \text{ dB re } 1 \text{ m}$ for impulse pressure). We chose the CPA shot RLs because it was the closest shot to the reference 1 m providing good SNR with the least amount of propagation loss, and its raypath was straight and direct without adverse refraction effects. Without closer range measurements and with water depths much greater than source/receiver propagation paths, spherical spreading is an appropriate propagation model for low frequency, omni-directional sources (Urick, 1983). Further supporting spherical spreading in this region was the transmission loss slope from CPA to ~340 m, measured to be $X = 20$ (Figure 7).

Seal bomb estimated peak SL of $234 \text{ dB}_p \text{ re } 1 \mu\text{Pa @ } 1 \text{ m}$ is a high source sound pressure level in the ocean (e.g., Hildebrand, 2009), and while our measurements show pulses about five times less peaky and five times longer duration than the high explosive model (Figures 4 and 6), it is possible that nonlinear propagation with higher TL than spherical spreading occurred for seal bomb explosions at shorter ranges than measured in our experiment. Eq. 11 predicts Eqs. 8 – 10 are valid from the source out to about 100 m when using an 80% TNT-equivalent seal bomb charge weight. The expected TL in this nonlinear region is $X = 22.6$ (i.e., $20\log_{10}(p_0)$, where $\alpha = 1.13$ in Eq. 8). Using this TL coefficient for the nonlinear region from 1 to 100 m and spherical spreading coefficient $X = 20$ for the linear region from 100 to 262 m, the total TL from the CPA shot would be $\text{TL} = 22.6\log_{10}(100) + 20\log_{10}(262/100) \approx 54 \text{ dB re } 1 \text{ m}$, or 6 dB more lossy than just spherical spreading suggesting the peak SL could be as high as $240 \text{ dB}_p \text{ re } 1 \mu\text{Pa @ } 1 \text{ m}$.

While little is known about damage to marine mammals from underwater explosions, the seal bomb source impulse SPL of $83 \text{ dB re } 1 \mu\text{Pa}\cdot\text{s @ } 1 \text{ m}$ ($200 \text{ Pa}\cdot\text{s @ } 1 \text{ m} = 29 \text{ psi}\cdot\text{ms @ } 3.2 \text{ ft}$) is within the realm of injury for medium-sized terrestrial animals held underwater (Yelverton *et al.*, 1973); however, using the nonlinear high explosive equations above (Eqs. 7 – 9) for an 80% TNT-equivalent seal bomb charge weight estimates a source impulse SPL of $80 \text{ dB re } 1 \mu\text{Pa}\cdot\text{s @ } 1 \text{ m}$ ($89 \text{ Pa}\cdot\text{s @ } 1 \text{ m} = 13 \text{ psi}\cdot\text{ms @ } 3.2 \text{ ft}$) or about a factor of two lower. This difference, similar to the 2 dB difference at 262 m, is primarily due to the wider pulse width and therefore larger area under the seal bomb measured pulse than the TNT-equivalent derived pulse.

Table 5. Source SPL and SEL estimates from seal bomb with charge weight of 2.33 g.

Metric	Levels
Peak Source SPL	234 ($\text{dB}_p \text{ re } 1 \mu\text{Pa @ } 1 \text{ m}$)
rms-3dB Source SPL	233 ($\text{dB}_{\text{rms}} \text{ re } 1 \mu\text{Pa @ } 1 \text{ m}$)
rms-10dB Source SPL	230 ($\text{dB}_{\text{rms}} \text{ re } 1 \mu\text{Pa @ } 1 \text{ m}$)
rms90% Source SPL	226 ($\text{dB}_{\text{rms}} \text{ re } 1 \mu\text{Pa @ } 1 \text{ m}$)
Impulse Source SPL	83 ($\text{dB re } 1 \mu\text{Pa}\cdot\text{s @ } 1 \text{ m}$)
Source SEL	197 ($\text{dB re } 1 \mu\text{Pa}^2\cdot\text{s @ } 1 \text{ m}$)

Discussion and Conclusions

To characterize seal bomb sound pressure signatures, we recorded calibrated underwater received levels of shots ranging from approximately 0.25 – 9 km and found the environment (i.e., temperature profile), and therefore season, had a significant effect on sound propagation for near sea surface sources due to raypath refraction or bending. This is an important point to consider when estimating SPL at a receiver from a known source, and *vice versa* as done here, estimating source SPL from received levels. For example, in the acoustically refractive model with source at 3 meters depth (Figure 9a), a receiver near the sea surface and ~500 m range would not receive any direct raypaths, only steep angle rays reflected off of the seafloor; and received levels would be less than predicted by spherical spreading. Conversely, the same receiver ~100 m range may receive sound at higher levels than spherical because of raypath focusing, and waveforms would likely be complicated with constructive and destructive interference from sea surface reflections due to low grazing angles both from source and to receiver at shallow depths.

Accounting for the propagation environment, we based our estimated seal bomb source peak sound pressure level on the closest shot's received level and a spherical spreading propagation loss model. Estimated SL were sufficiently high to question whether nonlinear propagation loss, as observed with high explosives such as TNT, may be present closer to the source than measured during this experiment. If seal bomb explosions are more like high explosive high-speed detonations than much slower deflagrates such as black powder, then we may have underestimated source sound pressure levels by up to 6 dB, or a factor of 2, prompting the need for a smaller scale follow-on experiment.

Peak and rms SPL are often used to describe underwater signals; however, they are incomplete for characterizing impulsive signals such as explosions, because no information on pulse shape is provided. Pulse duration provides additional details on the amount of energy contained in the pulse and the rate at which it is released. Time-integrated metrics impulse SPL and SEL are more comparable for impulsive signals because they account for the total energy in the pulse, not just the pressure amplitude. Seal bomb source (i.e., at 1 m range) impulse SPL was estimated to be at levels previously shown to cause injury to medium-size terrestrial mammals, but at lower levels than predicted for a TNT-equivalent weight charge using nonlinear high explosive equations owing to pulse width differences.

Furthermore, the complete waveform, not just the first pulse, of a seal bomb shot should be considered when evaluating impact because of the additional impulsive sounds present from explosion bubble pulses and reflections off the sea surface. Also, the total energy received is higher when the complete waveform is considered as integrating over the full 100 ms time window of Figure 5, results in an estimated source SEL of 203 dB re $1 \mu\text{Pa}^2 \cdot \text{s}$ @ 1m that is 6 dB higher than only the first pulse. Expanding one step further, calculating cumulative SEL over the full period of event activity would provide the total amount of sound energy emitted into the environment.

Acknowledgements

We thank Brett Pickering, the captain of Scripps Institution of Oceanography's R/V Saikhon, who provided excellence in planning, logistics, and execution of various operation at-sea and port. We thank Ryan Griswold and Bruce Thayre for their high-quality work and attention to detail with instrumentation maintenance, preparation, and use. Erin O'Neill we thank for her efficient and thorough management and execution of the data processing, quality-control and archiving operations required for the data set used here. We thank Erin Oleson and Amy Scholik-Schlomer from the National Oceanic and Atmospheric Administration (NOAA) National Marine Fisheries Service for their support of this project. Funding also was provided by Okeanos Foundation for the Sea, for which we thank Dieter Paulmann.

References

- Arons, A. B. (1954). "Underwater explosion shock wave parameters at large distances from the charge," *J Acoust Soc Am* **26**, 343-346.
- Arons, A. B., R., Y. D., and Cotter, T. P. (1949). "Long range shock propagation in underwater explosion phenomena II," in *U.S. Navy Dept. Bur. Ord. NAVORD Rep.* 478.
- Beyer, R. T. (1974). *Nonlinear Acoustics* (Brown University, Dept of Physics, Providence, RI), p. 405.
- Cassano, E. R., Myrick, A. C., Glick, C. B., Holland, R. C., and Lennert, C. E. (1990). "The use of seal bombs on dolphins in the eastern tropical Pacific yellowfin tuna purse-seine fishery," in *Administrative report LJ-90-09* (Southwest Fisheries Center, National Marine Fisheries Service, La Jolla, CA 92038).
- Chen, C.-T., and Millero, F. J. (1977). "Speed of sound in seawater at high pressures," *The Journal of the Acoustical Society of America* **62**, 1129-1135.
- Cole, R. H. (1948). *Underwater Explosions* (Princeton University Press, New Jersey), p. 437.
- Finneran, J. J. (2015). "Noise-induced hearing loss in marine mammals: A review of temporary threshold shift studies from 1996 to 2015," *The Journal of the Acoustical Society of America* **138**, 1702-1726.
- Hildebrand, J. A. (2009). "Anthropogenic and natural sources of ambient noise in the ocean," *Marine Ecology Progress Series* **395**, 5-20.
- Madsen, P. T. (2005). "Marine mammals and noise: Problems with root mean square sound pressure levels for transients," *Journal of the Acoustical Society of America* **117**, 3952-3957.
- Meyer-Löbbecke, A., Debich, A. J., Širović, A., Trickey, J. S., Roch, M. A., Carretta, J. V., Fraiser, K., Wiggins, S. M., Hildebrand, J. A., Denzinger, A., Schnitzler, H.-U., and Baumann-Pickering, S. (2016). "Noise from explosive deterrents used by California fisheries and possible effects on marine life (poster)," in *4th International Conference on the Effects of Noise on Aquatic Life, July10-16, 2016* (Dublin, Ireland).
- Myrick, A. C., Cassano, E. R., and Oliver, C. W. (1990a). "Potential for physical injury, other than hearing damage, to dolphins from seal bombs used in the yellowfin tuna purse-seine fishery: results from open-water tests," in *Administrative report LJ-90-07* (Southwest Fisheries Center, National Marine Fisheries Service, NOAA, La Jolla, California 92038).
- Myrick, A. C., Fink, M., and Glick, C. B. (1990b). "Identification, chemistry, and behavior of seal bombs used to control dolphins in the yellowfin tuna purse-seine fishery in the eastern tropical Pacific: potential hazards," in *Administrative report LJ-90-08* (Southwest Fisheries Center, National Marine Fisheries Service, La Jolla, CA 92038).
- Porter, M. B. (2011). "The BELLHOP manual and user's guide: preliminary draft," in (Heat, Light, and Sound Research, Inc., La Jolla, CA).
- Richardson, W. J., Greene, C. R., Malme, C. I., and Thomson, D. H. (1995). *Marine mammals and noise* (Academic Press, San Diego), p. 576.
- Southall, B. L., Bowles, A. E., Ellison, W. T., Finneran, J. J., Gentry, R. L., Greene, C. R., Kastak, D., Ketten, D. R., Miller, J. H., Nachtigall, P. E., Richardson, W. J., Thomas, J. A., and Tyack, P. L. (2007). "4. Criteria for Behavioral Disturbance," *Aquatic Mammals* **33**, 446-473.
- Urick, R. J. (1983). *Principles of underwater sound* (McGraw-Hill, New York), p. 423.

- Wiggins, S. M., and Hildebrand, J. A. (2007). "High-frequency Acoustic Recording Package (HARP) for broad-band, long-term marine mammal monitoring," in *International Symposium on Underwater Technology 2007 and International Workshop on Scientific Use of Submarine Cables & Related Technologies 2007* (IEEE, Tokyo, Japan), pp. 551-557.
- Yelverton, J. T., Richmond, D. R., Fletcher, E. R., and Jones, R. K. (1973). "Safe distances from underwater explosions for mammals and birds," in *DNA 3114T* (Rep. from Lovelace Foundation For Medical Education and Research Albuguerque, NM, for Defence Nuclear Agency, Washington, DC, 67p, NTIS AD-766952).